Chemistry & Biology
Article

Ralfuranone Biosynthesis in *Ralstonia solanacearum* Suggests Functional Divergence in the Quinone Synthetase Family of Enzymes

Barbara Wackler,[1] Patrick Schneider,[1] Jonathan M. Jacobs,[2] Julia Pauly,[1] Caitilyn Allen,[2] Markus Nett,[3] and Dirk Hoffmeister[1,*]
[1]Department Pharmaceutical Biology at the Hans-Knöll-Institute, Friedrich-Schiller-Universität Jena, Beutenbergstrasse 11a, 07745 Jena, Germany
[2]Department of Plant Pathology, University of Wisconsin-Madison, 1630 Linden Drive, Madison, WI 53706, USA
[3]Leibniz Institute for Natural Product Research and Infection Biology—Hans-Knöll-Institute, Beutenbergstrasse 11a, 07745 Jena, Germany
*Correspondence: dirk.hoffmeister@hki-jena.de
DOI 10.1016/j.chembiol.2011.01.010

SUMMARY

Ralstonia solanacearum **is a destructive crop plant pathogen and produces ralfuranone, i.e., a monophenyl-substituted furanone. Extensive feeding experiments with ^{13}C-labeled L-phenylalanine now proved that all carbon atoms of the heterocycle derive, after deamination, from this aromatic amino acid. A genetic locus was identified which encodes the aminotransferase RalD and the furanone synthetase RalA. The latter is a tridomain nonribosomal peptide synthetase (NRPS)-like enzyme which was characterized (1) biochemically by the ATP-pyrophosphate exchange assay, and (2) genetically through gene inactivation and transcriptional analysis in axenic culture and in planta. This is the first study to our knowledge on the biochemical and genetic basis of *R. solanacearum* secondary metabolism. It implies new chemistry for NRPSs, as RalA-mediated biosynthesis requires C-C-bond and subsequent C-O-bond formation to establish the furanone ring system.**

INTRODUCTION

The Gram-negative bacterium *Ralstonia solanacearum* is a notorious plant pathogen which invades its hosts in the rhizosphere and colonizes their xylem vessels, eventually leading to wilt disease (Hayward, 1991). Its epithet implies a dependence on solanaceaous plants, and, in fact, *R. solanacearum* threatens the health of agriculturally and commercially relevant crop plants within this family, such as tomato and potato. However, this bacterium also parasitizes numerous species of other mono- and dicotyledonous plant families including species of importance for staple food production, such as banana (Hayward, 1991). Given its significance as a crop plant pathogen, it is surprising that data on its secondary metabolome have only begun to emerge. One report is pertaining to biosynthesis and regulation of 3-hydroxy-oxindole (Delaspre et al., 2007). More recently, crosstalk between the global virulence regulators VsrAD and PhcA, and secondary metabolism has been demonstrated and led to the identification of a new small molecule, ralfuranone (4-phenylfuran-2(5*H*)-one, **1,** Figure 1) (Schneider et al., 2009). Although achiral and little functionalized, this bicyclic secondary product attracted our attention as the origin of the carbon atoms was elusive. Initially, we hypothesized that the aromatic system may be derived from L-phenylalanine, and that transfer of malonyl-CoA to the former may provide the carbon atoms to complete furanone synthesis. Chemical characterization of a new, yet related natural product, ralfuranone B (**2,** Figure 1), prompted us to propose a revised biosynthetic mechanism. Support came from feeding experiments with ^{13}C-labeled L-phenylalanine and from the genetic and biochemical characterization of two biosynthesis enzymes, the aminotransferase RalD and the furanone synthetase RalA. The latter is a tridomain protein reminiscent of fungal quinone synthetases and shares an identical domain architecture and a high degree of similarity with AtrA from the basidiomycete *Tapinella panuoides* (Schneider et al., 2008). However, our data on RalA imply a mechanism for furanone biosynthesis, which is dissimilar from quinone synthetase.

RESULTS AND DISCUSSION

Feeding Experiments

Stable isotope feeding was initiated with 1 mM [1,2-$^{13}C_2$] acetate as carbon source to probe its metabolic fate in the biosynthesis of **1**. Unexpectedly, *R. solanacearum* failed to produce **1** under these conditions. Therefore, we fed 1 mM [2-^{13}C] pyruvate to the bacterium, as genomic data supported an intracellular conversion into acetyl-CoA via the pyruvate dehydrogenase multienzyme complex. Albeit production of **1** could be restored in this way, no ^{13}C enrichment was detected at C-2 (or any other carbon atom) disproving our initial assumption that acetate serves as a building block. Concurrently, **2** was isolated from the culture broth of *R. solanacearum*. Its chemical structure is new, yet strongly resembling the fungal gymnoascolides (Figure 1) (Clark et al., 2005). A related compound, 3-carboxy-2,4-diphenyl-but-2-enoic anhydride (Figure 1), was also described as a fungal metabolite (Hamasaki and Nakajima, 1983). Combined with the results of the feeding experiment, the structure of **2** made us reconsider our working hypothesis on the origin of the

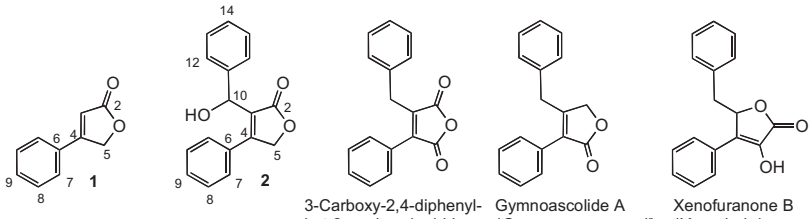

Figure 1. Chemical Structures of *Ralstonia* Metabolites Ralfuranone (1) and Ralfuranone B (2), and Related Natural Products of Other Sources

1 furanone carbons. The broad-band ^{1}H-decoupled ^{13}C NMR spectrum of **1** labeled from a feeding experiment with [U-$^{13}C_9$] L-phenylalanine indicated extensive enrichment and coupling throughout the molecule (see Figure S1 available online). For quantitative purposes, the absolute ^{13}C enrichment of the methylene carbon atom at C-5 was determined by integration of the methylene proton signal and its ^{13}C satellites in the ^{1}H NMR spectrum. The integral of the corresponding ^{13}C signal in the inverse gated ^{1}H-decoupled ^{13}C NMR spectrum was then used as the reference against which enrichments at other carbon atoms were calculated (Table 1). First order multiplet analysis in the ^{13}C NMR spectrum suggested an assembly of **1** from two discrete phenylalanine-derived fragments, that is, a C_6-C_2 moiety covering the carbon atoms C-4 to C-9 of ralfuranone and a C_2 unit composed of the remaining carbon atoms C-2 and C-3, respectively. This was further corroborated by consistent ^{13}C-enrichments within the C_6-C_2 versus C_2 building block (Table 1). As both fragments exhibit high enrichment levels, we assume that they derive intact without extensive modification from the fed precursor. Moreover, it appears plausible that **2** precedes the formation of **1**, and that a debenzylation reaction could give rise to the latter. C-2 and C-3 would thus originate from the carboxyl and the α-carbon in L-phenylalanine, respectively. Consistent with this assumption, administration of [3-^{13}C] L-phenylalanine (230 μM final) resulted in the exclusive incorporation of label at C-4.

Ralfuranone Biosynthesis Genes

Our results demonstrate that all carbon atoms of **1** are derived from L-phenylalanine and imply that a potential genetic locus encodes an enzyme to activate L-phenylalanine or, in conjunction with aminotransferase activity, phenylpyruvate. A multigene locus which meets these requirements was found around gene *RSp1419* on the megaplasmid of the published genome of *R. solanacearum* strain GMI1000 (Salanoubat et al., 2002). Located downstream of genes for flagellar motor proteins, i.e., proteins required for chemotaxis, and their transcriptional regulators, the gene *RSp1419* codes for a 937 amino acid (aa) putative tridomain monomodular nonribosomal peptide synthetase (NRPS)-like protein, including adenylation, thiolation, and thioesterase (A-T-TE) domains (Figure 2). Highest homologies of *RSp1419* were found to orthologs in the genomes of numerous *Burkholderia* isolates, including the etiological agent of melioidosis, *B. pseudomallei* (Wiersinga et al., 2006), and *B. oklahomensis* (Glass et al., 2006) (Table S1). Intriguingly, the protein RSp1419 showed remarkable cross-domain similarity to the fungal quinone synthetases TdiA and AtrA (34% and 39% identical aa, respectively (Balibar et al., 2007; Schneider et al., 2007, 2008). Their genes are located in loci which include aromatic aminotransferase genes (*tdiD* and *atrD*, respectively). A putative aminotransferase gene, *RSp1424/ectB*, coding for a 434 aa enzyme and annotated as diaminobutyrate:2-oxoglutarate transaminase gene, was present in the vicinity of *RSp1419* as well (Figure 2). Consequently, these two genes, hereafter referred to as *ralA* and *ralD* (GenBank accession: HQ864831 and HQ864832, respectively) were inactivated. The aminotransferase RalD was not strictly required for ralfuranone synthesis, as production was still active in a *ralD* disruption mutant, albeit at a reduced level (Figure 3). A very similar effect was found with terrequinone biosynthesis upon aminotransferase *tdiD* gene knockout, where production was impaired, but not abolished, possibly due to a partial complementation by housekeeping aminotransferases (Schneider et al., 2007). Mutants in which *ralA* was disrupted by a kanamycin resistance cassette completely lost the capacity to produce ralfuranone (Figure 3). Therefore, we conclude that RalA plays an essential role for ralfuranone biosynthesis. Although the ecological role of ralfuranone biosynthesis has not been clarified yet, a genetic screen found that *R. solanacearum* expresses *ralA* in planta (Brown and Allen, 2004). Gene expression analysis with DNA microarrays also identified that both *ralA* and *ralD* are highly expressed during wilt disease of tomato and in rich medium (Table 2) (Jacobs et al., 2010). The *ralA* gene is embedded in an apparently larger locus of putative natural product genes that implies more complex metabolites than just ralfuranones. However, these products have not been detected yet. In particular, the presence of *RSp1422*, located between *ralA* and *ralD* (Figure 2) and encoding a monomodular NRPS is incompatible with the structure of **1** and **2**, respectively, as neither has a peptide bond. Notably, *RSp1422* is moderately and slightly expressed in rich medium and in planta, respectively. This

Table 1. ^{13}C Abundance and Coupling Constants in Ralfuranone (1) Biosynthesized from ^{13}C-Labeled Precursors (125 MHz, CD_3OD; chemical shifts are referenced to CHD_2OD at 49.0 ppm)

Carbon atom	δ (ppm)	^{13}C-enrichment (%) ($^{1}J_{CC}$, Hz)[a]	
		[U-^{13}C] L-phenylalanine	[3-^{13}C] L-phenylalanine
2	176.8	63 (68)	
3	113.3	63 (68)	
4	167.2	59 (65, 36)	66
5	73.0	60 (36)	
6	131.2	59 (65, 59)	
7	128.0	59 (59, 54)	
8	130.3	59 (54)	
9	132.9	59 (54)	

[a] Signals for which no figures are given did not show significant enrichment.

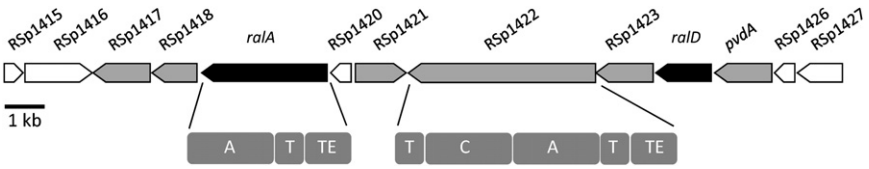

Figure 2. Physical Map of Ralfuranone Biosynthesis Genes *ralA* and *ralD* and Adjacent Reading Frames

Open arrows represent hypothetical genes; gray arrows represent putative natural product biosynthesis and transporter genes (details in Table S1). The layout of multidomain enzymes is shown below their genes. A, adenylation domain; C, condensation domain; T, thiolation domain; TE, thioesterase domain. For clarity, the domain order within the enzymes is shown in opposite direction to the transcriptional orientation of the gene.

differential regulation further supports that *RSp1422* serves a diverging biochemical pathway. Using the NRPSpredictor algorithm (Rausch et al., 2005) the anticipated substrate of RSp1419 is a salicylate-like (i.e., not an amino acid) molecule. Conversely, as a substrate for the RSp1422 A-domain, the same software expected an aliphatic amino acid, most likely valine. Such a specificity is not consistent with ralfuranone biosynthesis and suggests, too, a role within a diverging pathway. Final evidence came from a gene inactivation experiment. A strain in which *RSp1422* had been replaced by a dysfunctional copy produced ralfuranones at normal titers (Figure 3). The scenario of one gene cluster encoding the synthesis of two distantly related products is reminiscent, to a degree, to the recently described situation for rifamycin and saliniketal assembly in *Salinispora arenicola* (Wilson et al., 2010).

Enzyme Characterization

The gateway enzymes RalA and RalD were heterologously overexpressed in *Escherichia coli* as N-terminal hexahistidine fusion proteins. To confirm it uses a C_6-C_3-backbone as substrate we characterized apo-RalA using the ATP-pyrophosphate exchange assay and included phenylpyruvic acid, 4-hydroxyphenylpyruvic acid, L-phenylalanine, and cinnamic acid as potential building blocks. Further, the C_6-C_2 building blocks phenylglyoxylic acid, racemic mandelic acid, racemic phenylglycine, and phenylacetic acid were tested, along with pyruvic acid and L-alanine for control. Maximum turnover was found with phenylpyruvate, and, in second place, with 4-hydroxyphenylpyruvate (74% compared with phenylpyruvate, Figure 4). All other compounds tested were not turned over at a rate >5% confirming that, in fact, a C_6-C_3-precursor enters the RalA-mediated pathway. As is the case for fungal quinone synthetases, an aminotransferase is required to provide the proper substrate: chromatographically analyzed enzymatic assays of RalD identified this protein as a L-phenylalanine aminotransferase. In the presence of PLP the turnover to phenylpyruvate (the RalA substrate) was observed at a comparable rate with both pyruvate, imidazol-5-yl-pyruvate and 4-hydroxy-phenylpyruvate as amino acceptors, which is consistent with the substrate range of previously characterized aminotransferases (Minatogawa et al., 1977; Schneider et al., 2008). All other proteinogenic amino acids or their corresponding 2-oxo-counterparts failed as substrates. Therefore, the automatic genome annotation (*ectB*, diaminobutyrate:2-oxoglutarate transaminase) seems erroneous and does not reflect the true function of the gene and its product.

Biosynthetic Model

Consolidating chemical, genetic, and biochemical evidence, our model to explain **1** biosynthesis includes RalD-catalyzed

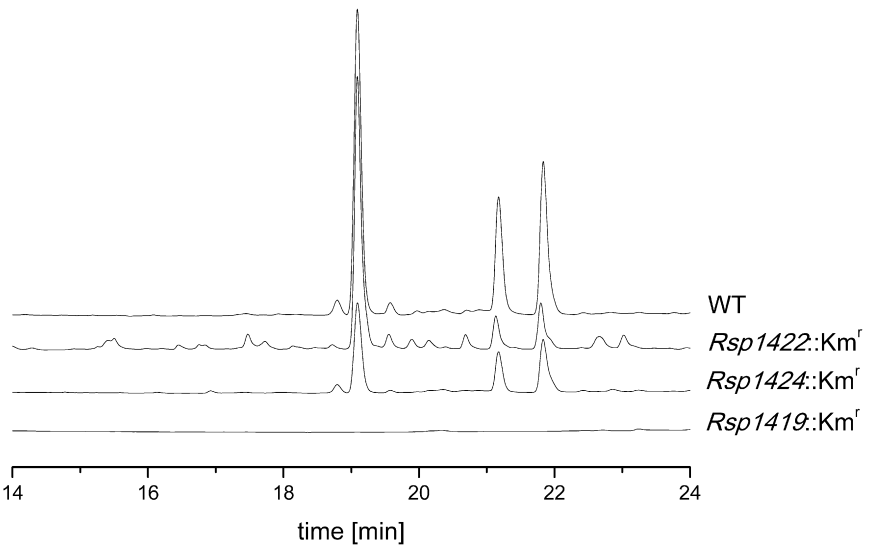

Figure 3. HPLC Chromatograms of *R. solanacearum* Crude Extracts

Wild-type strain GMI 1000 (WT), and the *ralA*, *RSp1422*, and *ralD* knockout strains (*RSp1419*::Km^r, *RSp1422*::Km^r, and *RSp1424*::Km^r). The signals at 19.2 and 21.3 min represent ralfuranone and ralfuranone B, respectively. The peak at 22.0 min corresponds to a hydroxylated ralfuranone derivative (*m/z* 176) described in (Schneider et al., 2009).

Table 2. Expression Patterns of *ralA*, *ralD*, and *RSp1422* in Rich Medium and during Wilt Disease of Tomato

Gene	Absolute $\log_2$ expression[a]	
	CPG Rich Medium	In Planta
ralA	13.8	14.5
ralD	13.3	11.9
RSp1422	8.0	6.8

[a] RNA for microarray analysis was collected from cells either grown to a cell density of approximately 6×10^8 CFU/ml in CPG rich medium (Hendrick and Sequeira, 1984) or bacteria at comparable cell density ($\sim 6 \times 10^8$ CFU/g stem) from tomato plants displaying 1%–25% wilting.

deamination of L-phenylalanine and loading of two molecules of phenylpyruvate onto the T- and TE-domains of RalA, respectively. A subsequent aldol condensation establishes a covalent bond between the α- and β-carbon atoms of the two building blocks (Figure 5). Mechanistic precedence for the latter reaction has been published by Boehlow et al. (1997). A nucleophilic attack on the carbonyl/thioester carbon then completes biosynthesis of the furanone heterocycle. Following the release from the TE domain, addition of water of the exocyclic double bond would allow for the elimination of benzaldehyde by a retro-aldol-cleavage. Finally, a decarboxylation reaction would give rise to **1**. It remains to be determined which of the post-RalA steps are enzyme-mediated or occur spontaneously. However, the gene *RSp1421* located between *ralA* and *ralD* and coding for a putative dehydratase would be consistent with a catalytic dehydratation. Ralfuranone B showed optical rotation, suggesting a chiral molecule which, in turn, points to a catalytic hydratation of the exocyclic double bond.

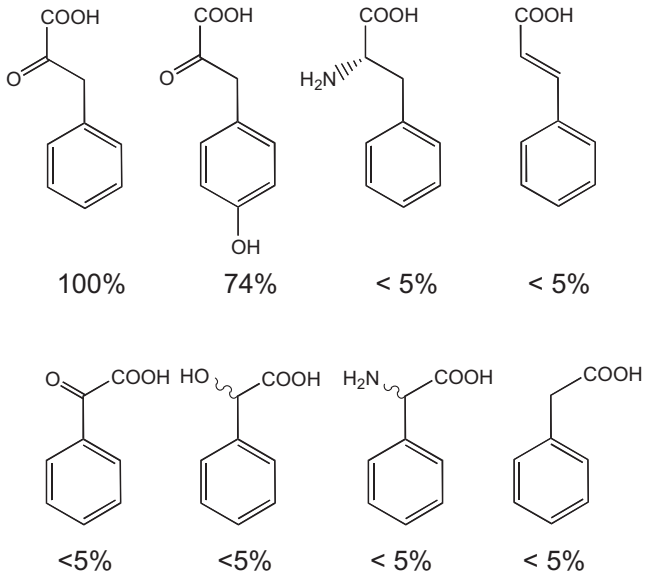

Figure 4. Potential RalA A-Domain Substrates Tested with the ATP-Pyrophosphate Exchange Assay

Relative activities are referenced to phenylpyruvic acid turnover. Upper row (left to right): phenylpyruvic acid, 4-hydroxyphenylpyruvic acid, L-phenylalanine, and cinnamic acid, lower row (left to right) phenylglyoxylic acid, mandelic acid, phenylglycine, and phenylacetic acid.

The central enzyme, RalA, is composed of three NRPS-domains A-T-TE but lacking a condensation domain. Therefore, RalA does not follow the standard composition of an NRPS module which would also include a condensation domain to catalyze the formation of a peptide bond (Schwarzer et al., 2003). Identically organized and seemingly incomplete monomodular NRPS, AtrA and TdiA, were found in fungi and have been identified as quinone synthetases (Schneider et al., 2007, 2008). The accepted model for AtrA/TdiA-mediated quinone formation includes symmetric formation of two carbon-carbon bonds between the carbonyl and β-carbon atoms of the two covalently bound building monomeric blocks (indole-3-pyruvate in the case of asterriquinones, 4-hydroxyphenylpyruvate for atromentin biosynthesis), via Claisen- and Dieckmann-type condensation reactions. The second reaction completes quinone formation thereby releasing the product from the enzyme. The model for ralfuranone biosynthesis, proposed here, implies a mechanism dissimilar from AtrA/TdiA and also new chemistry for NRPSs, and quinone synthetases in particular, as the RalA catalytic cycle includes formation of (1) one carbon-carbon bond between the β-carbon of the TE-bound and the α-carbon of the thioester-coupled monomer as well as (2) a carbon-oxygen bond, to establish the heterocycle. Beyond ralfuranone, the biochemistry described here may represent a more widespread mechanism and explain, e.g., xenofuranone biosynthesis (Figure 1) (Brachmann et al., 2006).

In summary, the combined data of gene inactivation, microarray results, feeding of labeled precursors, and biochemical characterization of RalA showed that the capacity of tridomain natural product enzymes with an A-T-TE domain setup reaches beyond quinone synthetase activity and that they are functionally more diverse than previously evident. We conclude RalA serves as a furanone synthetase, a new member of a further emerging class of natural product enzymes. Our results also shed more light on *Ralstonia solanacearum* natural products and may help understand the ecological relevance of the secondary metabolism of this important plant pathogen.

SIGNIFICANCE

In this first study, to our knowledge, on the biochemical and genetic basis of the secondary metabolism in *Ralstonia solanacearum*, we describe identification of the first furanone synthetase, RalA. Its primary amino acid sequence and domain organization is highly similar to fungal quinone synthetases, which consist of three distinct domains and which dimerize aromatic 2-oxo acids into quinone natural products by symmetric carbon-carbon-bond formation. As furanone synthesis occurs via carbon-carbon- and carbon-oxygen-bond formation, our results on RalA imply a mechanism dissimilar from quinone synthetase. *Ralstonia solanacearum* is a widely distributed bacterial plant pathogen. We noticed a strong disproportion between comprehensive genetic research on virulence while the secondary metabolism of this bacterium is remarkably little understood, thus contrasting efforts to elucidate pathogenicity mechanisms. Our results may therefore open the gate to investigate and understand the small molecule-based chemical ecology of a major crop plant pathogen. An

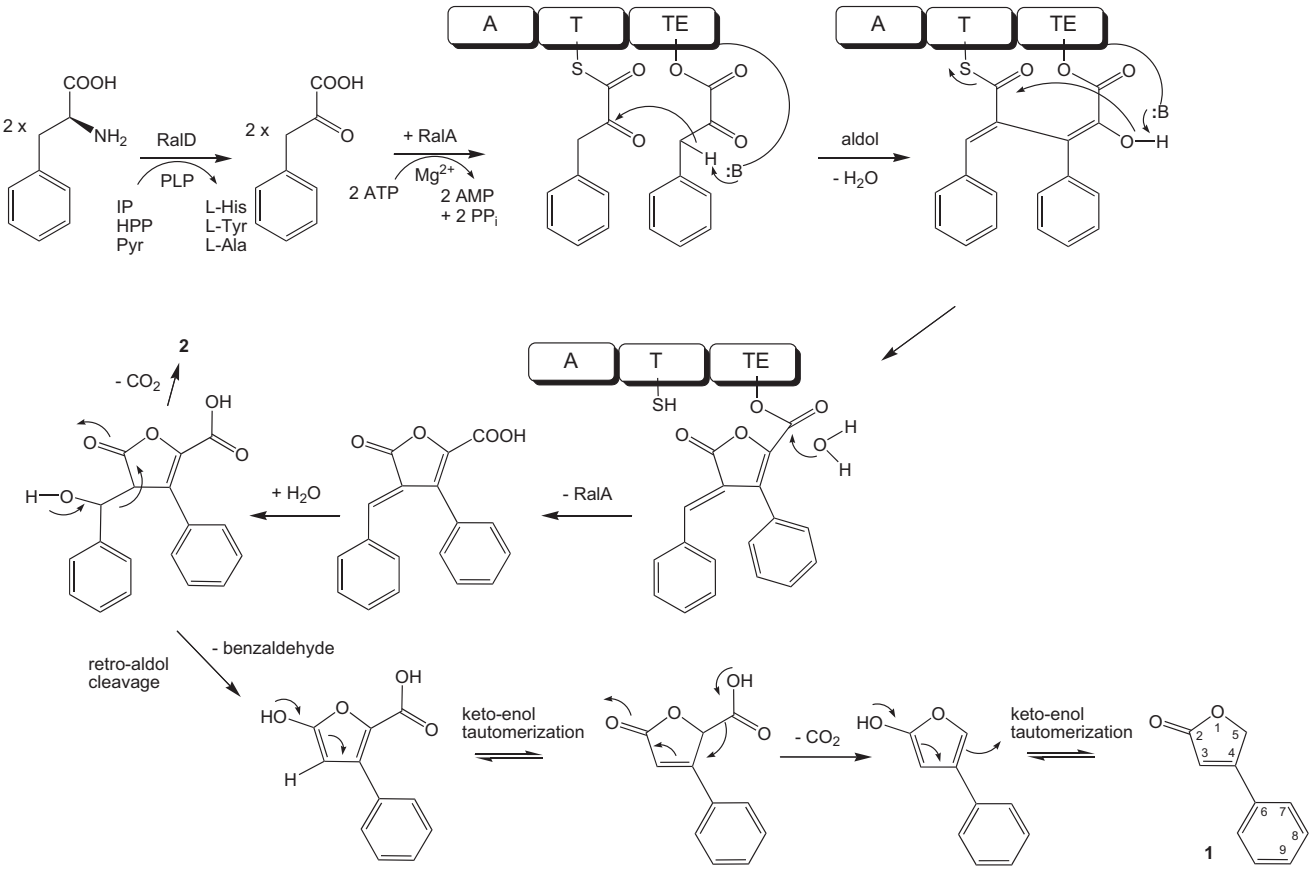

Figure 5. Proposed Route of Furanone Biosynthesis in *R. solanacearum*, Involving Aminotransferase and Furanone Synthetase Activity
IP, imidazol-5-yl-pyruvate; HPP, 4-hydroxyphenylpyruvate; Pyr, pyruvate. For stable isotope feeding experiment data, see Figure S1.

increasing number of microbial genomes is sequenced and browsed to discover new natural products or toxins. For the peptide synthetase family of enzymes, our results help annotate orphan natural product genes and predict biosynthetic capacities more accurately. Thus, imprecise designations during automatic genome annotation are avoided to make "mining" for new bioactive compounds more effective and straightforward.

EXPERIMENTAL PROCEDURES

Microbial Fermentation

R. solanacearum strains (GMI1000, wild-type), and knockout strains (*RSp1419*::Km^r, *RSp1422*::Km^r, *RSp1424*::Km^r), were routinely grown in liquid 1/4 × M63-Medium (Cohen and Rickenberg, 1956) with 10 mM sodium pyruvate as carbon source and supplemented with 2 mM L-phenylalanine (100 ml in 300 ml Erlenmeyer flasks), at room temperature and shaken at 180 rpm. ^{13}C feeding experiments were carried out in 1/4 × M63-medium amended with [1,2-$^{13}C_2$]acetate (1 mM final), [2-^{13}C] pyruvate (1 mM final), [3-^{13}C] L-phenylalanine (230 μM final), or [U-$^{13}C_9$] L-phenylalanine (120 μM final). To the latter two cultures 5 mM of unlabeled sodium pyruvate was added as principal carbon source. The culture volume was 8 liters in all four cases, shaken for 5 days at 28°C. Ralfuranone B (**2**) was isolated from a 28 liter fermentation (the medium was dispensed in approximately 1.5 liter portions in 3 liter Erlenmeyer flasks) harvested already after 3 days. Chemicals and media components were purchased from Becton Dickinson, Cambridge Isotope, Fisher, Roth, and Sigma-Aldrich.

Gene Inactivation

Constructs to inactivate the genes *RSp1419* and *RSp1424* in *R. solanacearum* GMI1000 were created by inserting PCR-amplified internal target gene fragments into the BamHI site of pST1-blue (Novagen). This restriction site was introduced into the PCR products by the oligonucleotide primers. The reactions (100 μl total volume each) were 2.5 mM $MgCl_2$, 0.2 mM each dNTP, 40 pmol each primer, and 3U Pfu DNA-polymerase. Thermal cycling conditions were: initial denaturation, 2 min, 94°C; amplification, 30 cycles (94°C for 40 s, 55°C for 30 s, 72°C for 3 min); terminal hold, 5 min at 72°C. Primers 1419KO-F (5′-TTGGATCCGCTGGTCTGTAGC-3′) and 1419KO-R (5′-TTCTGACGCACGGGATCCTGC-3′) amplified a 1434 bp fragment of *RSp1419*, while primers 1424KO-F (5′-CAACGGGATCCTCGACAAGGC-3′) and 1424KO-R (5′-ACAAGGATCCATCAGCAGACC-3′) were used for the 1077 bp fragment of *RSp1424*. This resulted in insertion mutation constructs *RSp1419*::*Kan*^{r} and *RSp1424*::*Kan*^{r}. The *RSp1422* disruption cassette was constructed by joining (1) a 1 kb DNA fragment including the 3′ region of *RSp1422* and 0.25 kb downstream of its stop codon (primers 1422A and 1422B, introducing a SpeI and a SmaI site, respectively), and (2) a 0.9 kb DNA fragment comprising the 5′ region and 0.5 kb of sequence upstream of the *RSp1422* start codon (primers 1422C and 1422D, introduced sites: SmaI and MfeI) with (3) the *aphA*-3 marker gene (Ménard et al., 1993). This construct was inserted via the MfeI and SpeI sites into pUFR80 (Ried and Collmer, 1987), cut by EcoRI and XbaI, to yield plasmid pJP37. Thermal cycling conditions to produce *RSp1422* inactivation cassette elements were: initial denaturation,

2 min, 95°C; amplification, 37 cycles (95°C for 30 s, 55°C for 30 s, 72°C for 1 min); terminal hold, 5 min at 72°C.

Primer sequences (introduced restriction sites underlined) are: 1422A: 5′-C GGCTCAGCCACTAGTCAACGCACCAG-3′; 1422B: 5′-CCCGGGGCATCGA GCTGGTGGCCTTCGATTC-3′; 1422C: 5′- CCAGCTCGATGCCCCGGGCGG TGAGTTCGAATGCAAGC-3′; 1422D: 5′- CTGACGCAATTGCTCGGCTACGC CGACTATC-3′.

Inactivation constructs were introduced by natural transformation, as previously described (Bertolla et al., 1997). Putative mutants were selected based on their respective antibiotic resistance, and verified by PCR and by their EPS-colony morphology. In the case of pJP37, additional selection for sucrose tolerance was carried out.

Enzyme Characterization

The genes *ralA* and *ralD* were amplified by PCR from *R. solanacearum* genomic DNA. The reaction (100 μl) was 2.5 mM $MgCl_2$, 0.2 mM each dNTP, 40 pmol each primer (1419NF and 1419NR for *ralA,* or 1424NF and 1424NR for *ralD*, respectively). Four units Pfu DNA-polymerase was added, and the following thermocycling parameters were used: initial denaturation, 3 min, 97°C; amplification, 30 cycles (95°C for 1 min, 60°C for 30 s, 72°C for 6 min); terminal hold, 9 min at 72°C (elongation time for *ralD* amplification: 4 min). Primer sequences are: 1419NF: 5′-GAACGACATATGACGACCGTAGCTG-3′, 1419NR: 5′-CCCC TGGATCCGGCTCACGCGGCATC-3′, 1424NF: 5′-GATCCATATGGACG TCTTTTCC-3′ 1424NR: 5′-GGATTGGATCCTTGCGCTCATGC-3′. PCR products were ligated to the NdeI/BamHI sites of pET28a (Novagen), to create plasmids pET28-RSp1419 and pET28-RSp1424, respectively, whose inserts were sequenced. Expression was accomplished in *E. coli* BL21 (DE3) × pLysS transformed with the above plasmids and as described earlier (Schneider et al., 2008). The RalA adenylation domain was characterized using the ATP-PP_i-exchange assay. All reactions were run in triplicate. Reaction parameters were: total volume of 100 μl at 37°C in 100 mM Tris-HCl buffer (pH 7.5), 5 mM $MgCl_2$, 5 mM ATP, 100 nM purified apo-RalA, 0.1 mM [^{32}P]-pyrophosphate, and 1 mM phenylpyruvate (or other substrates described in the text). The reaction proceeded for 30 min, before it was stopped and further processed as described (Van Lanen et al., 2005). The aminotransferase assay to characterize RalD followed a described procedure (Schneider et al., 2008).

Chemical Analysis

Five milliliters of liquid culture supernatant was extracted once with ethyl acetate, which was removed in vacuo. The extract was dissolved (methanol, 100 μl) and 10 μl injected. Analytical HPLC was performed on an Agilent 1200 instrument equipped with a Zorbax Eclipse XDB C-18 column (150 × 4.6 mm, 3.5 μm particle size) and a guard column. The following gradient was applied (solvent A: water, solvent B: acetonitrile): initial hold for 2 min at 15% B, then linear increase to 95% B over 20 min, at a flow rate of 0.5 ml/min. Chromatograms were recorded at λ = 258 nm. High-resolution mass spectrometry was accomplished on an Exactive Orbitrap instrument (Thermo Fisher), using electrospray ionization and the direct injection mode. NMR spectra were recorded on 500 MHz and 600 MHz Bruker Avance III spectrometers.

Labeled Compound Purification

^{13}C labeled ralfuranone (**1**) was obtained extracting the culture volume (8 liters) twice with an equal volume of ethyl acetate. The crude extract was dissolved in methanol, and purification done by preparative HPLC (Waters Autopurification System, equipped with an XTerra MS C-18 column, 50 × 19 mm, 5 μm particle size, flow at 20 ml min^{-1}, solvent A: 0.1% formic acid in H_2O, solvent B: methanol) which yielded 3.2 mg of **1**. The gradient was as follows: initial hold for 2 min at 5% B, followed by a linear increase to 100% B within 16 min.

Ralfuranone B (2) Preparation

The harvested 28 liter fermentation was extracted twice with an equal volume of ethyl acetate. After solvent evaporation under reduced pressure, the consolidated crude extracts were chromatographed on silica gel. Elution was achieved by a step gradient (25% increments) from 100% cyclohexane to 100% ethyl acetate, followed by a wash with 100% methanol. **2** eluted during the 50:50 cyclohexane: ethyl acetate step, and was purified to homogeneity by preparative HPLC under the conditions described above. Spectral data of **2**: $[\alpha]^{20}_D$ −7.9 (*c* = 0.1, MeOH); ^{1}H NMR (600 MHz, CD_3OD): δ (multiplicity assignment, coupling constants, position) 7.62 (d, *J* = 7.8 Hz, 2H, H-7 and H-7′), 7.49 (t, *J* = 7.2 Hz, 1H, H-9), 7.48 (t, *J* = 7.8, 7.2 Hz, 2H, H-8 and H-8′), 7.45 (d, *J* = 8.0 Hz, 2H, H-12 and H-12′), 7.33 (t, *J* = 8.0, 7.4 Hz, 2H, H-13 and H-13′), 7.26 (t, *J* = 7.4 Hz, 1H, H-14), 5.90 (s, 1H, H-10), 5.31 (d, *J* = 17.6 Hz, 1H, H-5a), 5.24 (d, *J* = 17.6 Hz, 1H, H-5b); ^{13}C NMR (150 MHz, CD_3OD): δ (position) 175.6 (C-2), 161.8 (C-4), 142.6 (C-11), 132.0 (C-6), 131.7 (C-9), 129.9 (C-8 and C-8′), 129.4 (C-7 and C-7′), 129.2 (C-13 and C-13′), 128.8 (C-3), 128.4 (C-14), 127.2 (C-12 and C-12′), 72.6 (C-5), 68.1 (C-10); HR-ESIMS (-) calcd for $C_{17}H_{13}O_3$: 265.0870, found 265.0877 $[M-H]^-$.

ACCESSION NUMBERS

DNA sequences of *ralA* and *ralD* have been deposited in GenBank under accession numbers HQ864831 and HQ864832, respectively.

SUPPLEMENTAL INFORMATION

Supplemental Information includes one figure and one table and can be found with this article online at doi:10.1016/j.chembiol.2011.01.010.

ACKNOWLEDGMENTS

Professor Dr. Wolfgang Steglich (Ludwig-Maximilians-Universität München, Germany) is gratefully acknowledged for valuable discussions. We thank Andrea Perner, Dr. Kirsten Scherlach, and Franziska Rhein (Leibniz Institute for Natural Product Research and Infection Biology - Hans-Knöll-Institute, Jena) for recording the high-resolution mass and NMR spectra of ralfuranone B, respectively. Support for this study from the University of Wisconsin-Madison College of Agricultural and Life Sciences to C.A., and from the Hans-Knöll-Institute to D.H., is gratefully acknowledged. We declare that we have no conflicting financial interests.

Received: September 8, 2010
Revised: December 31, 2010
Accepted: January 7, 2011
Published: March 24, 2011

REFERENCES

Balibar, C.J., Howard-Jones, A.R., and Walsh, C.T. (2007). Terrequinone A biosynthesis through L-tryptophan oxidation, dimerization and bisprenylation. Nat. Chem. Biol. *3*, 584–592.

Bertolla, F., van Gijsegem, F., Nesme, X., and Simonet, P. (1997). Conditions for natural transformation of *Ralstonia solanacearum*. Appl. Environ. Microbiol. *63*, 4965–4968.

Boehlow, T.R., Rath, N.P., and Spilling, C.D. (1997). Dimethyl (+/−)-(1S*,2R*,3S*)-[3-phenyl-1-(N-phenylcarbamoyloxy)-2,3-epoxypropyl]phosphonate. Acta Crystallograph. *C53*, 92–95.

Brachmann, A.O., Forst, S., Furgani, G.M., Fodor, A., and Bode, H.B. (2006). Xenofuranones A and B: Phenylpyruvate Dimers from *Xenorhabdus szentirmaii*. J. Nat. Prod. *69*, 1830–1832.

Brown, D.G., and Allen, C. (2004). *Ralstonia solanacearum* genes induced during growth in tomato: an inside view of bacterial wilt. Mol. Microbiol. *53*, 1641–1660.

Clark, B., Capon, R.J., Lacey, E., Tennant, S., Gill, J.H., Bulheller, B., and Bringmann, G. (2005). Gymnoascolides A-C: aromatic butenolides from an Australian isolate of the soil ascomycete *Gymnoascus reessii*. J. Nat. Prod. *68*, 1226–1230.

Cohen, G.N., and Rickenberg, H.V. (1956). La galactoside-perméase d' *Escherichia coli*. Ann. Inst. Pasteur (Paris) *91*, 693–720.

Delaspre, F., Nieto Peñalver, C.G., Saurel, O., Kiefer, P., Gras, E., Milon, A., Boucher, C., Genin, S., and Vorholt, J.A. (2007). The *Ralstonia solanacearum* pathogenicity regulator HrpB induces 3-hydroxy-oxindole synthesis. Proc. Natl. Acad. Sci. USA *104*, 15870–15875.

Glass, M.B., Steigerwalt, A.G., Jordan, J.G., Wilkins, P.P., and Gee, J.E. (2006). *Burkholderia oklahomensis* sp. nov., a *Burkholderia pseudomallei*-like species formerly known as the Oklahoma strain of *Pseudomonas pseudomallei*. Int. J. Syst. Evol. Microbiol. *56*, 2171–2176.

Hamasaki, T., and Nakajima, H. (1983). A new metabolite, 3-carboxy-2,4-diphenyl-but-2-enoic anhydride, produced by *Aspergillus nidulans*. Agric. Biol. Chem. *47*, 891–892.

Hayward, C.A. (1991). Biology and epidemiology of bacterial wilt caused by *Pseudomonas solanacearum*. Annu. Rev. Phytopathol. *29*, 65–87.

Hendrick, C.A., and Sequeira, L. (1984). Lipopolysaccharide-Defective Mutants of the Wilt Pathogen *Pseudomonas solanacearum*. Appl. Environ. Microbiol. *48*, 94–101.

Jacobs, J.M., Babujee, L., Meng, F., Milling, A., and Allen, C. (2010). Comparative *in planta* microarray analysis modifies the regulatory model for the type three secretion system in *Ralstonia solanacearum*. Phytopathology *100*, S55.

Ménard, R., Sansonetti, P.J., and Parsot, C. (1993). Nonpolar mutagenesis of the *ipa* genes defines IpaB, IpaC, and IpaD as effectors of *Shigella flexneri* entry into epithelial cells. J. Bacteriol. *175*, 5899–5906.

Minatogawa, Y., Noguchi, T., and Kido, R. (1977). Species distribution and properties of hepatic phenylalanine (histidine):pyruvate aminotransferase. Hoppe Seylers Z. Physiol. Chem. *358*, 59–67.

Rausch, C., Weber, T., Kohlbacher, O., Wohlleben, W., and Huson, D.H. (2005). Specificity prediction of adenylation domains in nonribosomal peptide synthetases (NRPS) using Transductive Support Vector Machines (TSVM). Nucleic Acids Res. *33*, 5799–5808.

Ried, J.L., and Collmer, A. (1987). An *nptI-sacB-sacR* cartridge for constructing directed, unmarked mutations in gram-negative bacteria by marker exchange-eviction mutagenesis. Gene *57*, 239–246.

Salanoubat, M., Genin, S., Artiguenave, F., Gouzy, J., Mangenot, S., Arlat, M., Billault, A., Brottier, P., Camus, J.C., Cattolico, L., et al. (2002). Genome sequence of the plant pathogen *Ralstonia solanacearum*. Nature *415*, 497–502.

Schneider, P., Weber, M., Rosenberger, K., and Hoffmeister, D. (2007). A one-pot chemoenzymatic synthesis for the universal precursor of antidiabetes and antiviral bis-indolylquinones. Chem. Biol. *14*, 635–644.

Schneider, P., Bouhired, S., and Hoffmeister, D. (2008). Characterization of the atromentin biosynthesis genes and enzymes in the homobasidiomycete *Tapinella panuoides*. Fungal Genet. Biol. *45*, 1487–1496.

Schneider, P., Jacobs, J.M., Neres, J., Aldrich, C.C., Allen, C., Nett, D., and Hoffmeister, D. (2009). The global virulence regulators VsrAD and PhcA control secondary metabolism in the plant pathogen *Ralstonia solanacearum*. ChemBioChem *10*, 2730–2732.

Schwarzer, D., Finking, R., and Marahiel, M.A. (2003). Nonribosomal peptides: from genes to products. Nat. Prod. Rep. *20*, 275–287.

Van Lanen, S.G., Dorrestein, P.C., Christenson, S.D., Liu, W., Ju, J., Kelleher, N.L., and Shen, B. (2005). Biosynthesis of the beta-amino acid moiety of the enediyne antitumor antibiotic C-1027 featuring beta-amino acyl-S-carrier protein intermediates. J. Am. Chem. Soc. *127*, 11594–11595.

Wiersinga, W.J., van der Poll, T., White, N.J., Day, N.P., and Peacock, S.J. (2006). Melioidosis: insights into the pathogenicity of *Burkholderia pseudomallei*. Nat. Rev. Microbiol. *4*, 272–282.

Wilson, M.C., Gulder, T.A., Mahmud, T., and Moore, B.S. (2010). Shared biosynthesis of the saliniketals and rifamycins in *Salinispora arenicola* is controlled by the sare1259-encoded cytochrome P450. J. Am. Chem. Soc. *132*, 12757–12765.

